Failure Criteria Interpretation Based on Mohr-Coulomb Friction

By D. V. Griffiths[1]

Abstract: The use of numerical methods such as finite elements to make accurate predictions of failure or collapse of geomaterials must utilize a suitable failure criterion that is able to represent the shear strength for all stress paths likely to be encountered. The best-known failure criterion is that of Mohr-Coulomb, but several others have been proposed. Using a dimensionless form of principal stress space, this paper reviews some of these other criteria in a unified way by presenting them in terms of the equivalent Mohr-Coulomb friction angle implied at various locations on their periphery. Circular conical surfaces in stress space can greatly overestimate the strength of soil for certain stress paths, and sometimes contain singularities as implied by an equivalent friction angle of 90°. Noncircular conical surfaces have also been considered. These give a more acceptable range of equivalent friction angles, as they are based on actual test data. These "sophisticated" criteria can still predict equivalent friction angles that differ from each other by several degrees, however.

Introduction

Prediction of failure stresses for frictional soils has traditionally been based on the Mohr-Coulomb criterion, which remains the most widely used in geotechnical practice. The popularity of this model lies in its simplicity and conservatism, where, for cohesionless soils, failure is indicated when the principal stress ratio reaches a limiting value given by

$$R = K_p \quad \ldots\ldots (1)$$

where

$$R = \frac{\sigma_1}{\sigma_3} \quad \ldots\ldots (2)$$

$$K_p = \tan^2\left(45° + \frac{\phi_c'}{2}\right) \quad \ldots\ldots (3)$$

and ϕ_c' = friction angle measured in triaxial compression.

For more advanced applications, especially in a computational environment, the Mohr-Coulomb criterion has been criticized on the grounds that it takes no account of the intermediate principal stress σ_2. It is well known, for example, that the friction angle in plane strain can be several degrees higher than its triaxially measured counterpart. The friction angle in triaxial extension is also thought to be higher than in triaxial compression, although the former is more sensitive to the experimental technique used to obtain it, and is therefore less reliable.

The Mohr-Coulomb criterion, based on a strength test in triaxial compres-

[1]Sr. Lect. in Engrg., Simon Building, Dept. of Engrg., Univ. of Manchester, Manchester M13 9PL, England.

Note. Discussion open until November 1, 1990. To extend the closing date one month, a written request must be filed with the ASCE Manager of Journals. The manuscript for this paper was submitted for review and possible publication on February 24, 1988. This paper is part of the ***Journal of Geotechnical Engineering***, Vol. 116, No. 6, June, 1990. ©ASCE, ISSN 0733-9410/90/0006-0986/$1.00 + $.15 per page. Paper No. 24794.

sion, is undoubtedly conservative, and partly for this reason, more realistic failure criteria have been proposed, which take equal account of all three principal stresses. A further objection to the Mohr-Coulomb criterion has been made in relation to its shape in principal stress space, which takes the form of an irregular hexagonal cone with its apex at the origin. The shape of the surface and, particularly, the corners, leads to difficulties with certain numerical algorithms. It turns out however, that this particular difficulty is quite easily overcome by introducing a local rounding of the corners (Smith and Griffiths 1988).

Another problem with the Mohr-Coulomb criterion occurs in multisurface kinematic models (Mroz 1967; Prevost 1985), in which a set of similar nested surfaces are used to model the yielding of soil from first loading through failure. The straight sides of the Mohr-Coulomb surface in the deviatoric planes would lead to ambiguity over the point of tangency when two surfaces came into contact. Implementation of such models clearly requires the use of smooth convex surfaces.

When using the finite element method in two or three dimensions to compute collapse loads, the complex stress fields encountered have led analysts to seek more general failure criteria [see e.g., Humpheson (1976), Vermeer (1988), and Smith (1988)]. These criteria are broadly similar to Mohr-Coulomb, except they usually take equal account of all three principal stresses.

The purpose of this paper is to review some of the failure criteria that have been proposed as smooth alternatives to Mohr-Coulomb. The surfaces are dealt with in a unified way by expressing them in terms of the equivalent Mohr-Coulomb friction angle ϕ'_{mc}. The angle ϕ'_{mc} is defined as the angle of friction of the Mohr-Coulomb surface that would pass through the particular point under consideration. This approach enables direct comparisons to be made between different failure criteria using a familiar soil mechanics parameter. It is shown that some criteria can lead to serious over- and underestimations of the actual strength of soil, whereas others even contain singularities for certain stress paths.

Review of Stress Space and Stress Invariants

To study the general stress fields that occur in a complicated boundary value problem, it is convenient to use principal stress space, which also leads to a convenient geometric representation of various failure criteria. A stress point in principal stress space can be defined using the following invariants

$$(s,t,\theta) \quad (4)$$

where

$$s = \frac{1}{\sqrt{3}}(\sigma_1 + \sigma_2 + \sigma_3) \quad (5)$$

$$t = \frac{1}{\sqrt{3}}[(\sigma_1 - \sigma_2)^2 + (\sigma_2 - \sigma_3)^2 + (\sigma_3 - \sigma_1)^2]^{1/2} \quad (6)$$

$$\theta = \arctan\left[\frac{1}{\sqrt{3}}\frac{(\sigma_1 - 2\sigma_2 + \sigma_3)}{(\sigma_1 - \sigma_3)}\right] \quad (7)$$

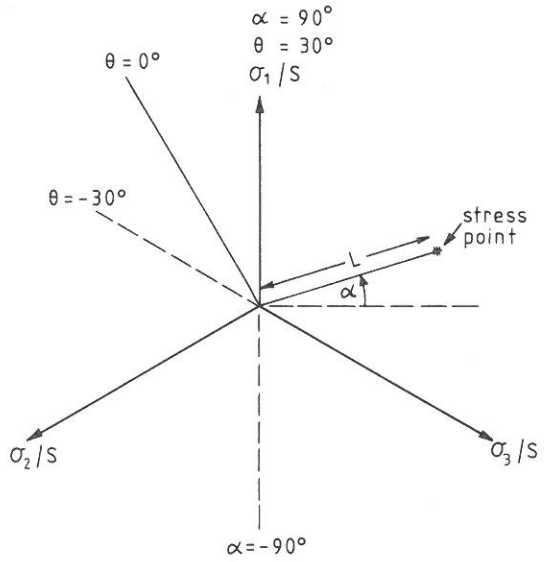

FIG. 1. Dimensionless Principal Stress Space

From Eqs. 4–7, s represents the perpendicular distance of the deviatoric plane containing the stress point from the origin, t represents the radial distance of the stress point from the space diagonal, and θ is the lode angle giving an angular measure of position within the deviatoric plane. In this context, the lode angle varies in the range

$$-30° \leq \theta \leq 30° \quad (8)$$

where $\theta = -30°$ corresponds to triaxial extension, and $\theta = 30°$ to triaxial compression. It is often useful to nondimensionalize principal stress space as shown in Fig. 1, by dividing all lengths by the invariant s leading to normalized coordinates

$$(1,L,\theta) \quad (9)$$

where

$$L = \frac{t}{s} \quad (10)$$

This overcomes any ambiguity over the sign convention, as it is recognized that the majority of geotechnical engineers use a compression-positive convention. Other invariants that will be used are the stress invariants, I_1, I_2, I_3. For completeness these are defined in the following.

$$I_1 = \sigma_1 + \sigma_2 + \sigma_3 \quad (11a)$$

$$I_2 = \sigma_1\sigma_2 + \sigma_2\sigma_3 + \sigma_3\sigma_1 \quad (11b)$$

$$I_3 = \sigma_1\sigma_2\sigma_3 \quad (11c)$$

Mohr-Coulomb Angle in Relation to Principal Stress Space

The equivalent Mohr-Coulomb friction angle ϕ'_{mc} corresponding to a particular location in stress space, can be found from invariants L and θ. Due to the corners on the Mohr-Coulomb surface, the general expression can be written in the form

$$\phi'_{mc} = \arcsin\left[\frac{\sqrt{3}L\cos\theta}{\sqrt{2} + L\sin\theta}\right] \quad \ldots\ldots (12)$$

where, with reference to Fig. 1 and taking account of symmetry about the σ_1/s axis:

$$\theta = \alpha + 60° \quad \text{if } -90° \le \alpha < -30° \quad \ldots\ldots (13a)$$

$$\theta = -\alpha \quad \text{if } -30° \le \alpha < +30° \quad \ldots\ldots (13b)$$

$$\theta = \alpha - 60° \quad \text{if } +30° \le \alpha \le +90° \quad \ldots\ldots (13c)$$

Circular Conical Criteria

These were among the earliest surfaces (Drucker and Prager 1952; Drucker et al. 1957) suggested as being suitable for representing the strength of soils. They project as circles in deviatoric planes, and are usually fitted exactly to Mohr-Coulomb's hexagon at certain locations on their circumference. Many circular fits are possible (Humpheson 1976; Zienkiewicz et al. 1978), but the three considered here are the limiting internal and external cones (Griffiths 1986), and an anisotropic cone (Prevost 1985), of the type that has been proposed in early versions of kinematic plasticity models for frictional soil.

External Cone

Referring to Fig. 2, the external cone is fitted to the Mohr-Coulomb criterion at the apexes of the hexagon corresponding to triaxial compression. When viewed in a deviatoric plane the circle is centered at the origin with a radius given by

$$L = \frac{2\sqrt{2}\sin\phi'_c}{3 - \sin\phi'_c} \quad \ldots\ldots (14)$$

where ϕ'_c is the friction angle of the circumscribed Mohr-Coulomb surface. Substituting L into Eq. 12 gives the following expression relating the equivalent friction angle ϕ'_{mc} to the angular invariant θ.

$$\phi'_{mc} = \arcsin\left[\frac{2\sqrt{3}\sin\phi'_c\cos\theta}{3 + \sin\phi'_c(2\sin\theta - 1)}\right] \quad \ldots\ldots (15)$$

Due to the sixfold symmetry in stress space, this relationship is illustrated in Fig. 3 over a 60° sector of principal stress space for three external cones fitted to ϕ'_c = 25°, 30°, and 36.87°. As expected $\phi'_{mc} = \phi'_c$ for triaxial compression stress paths (θ = 30°), however, considerable overestimates of strength can occur for other stress paths. For example, a cone fitted at ϕ'_c = 30° could predict an equivalent friction angle ϕ'_{mc} as high as 49.11° for a

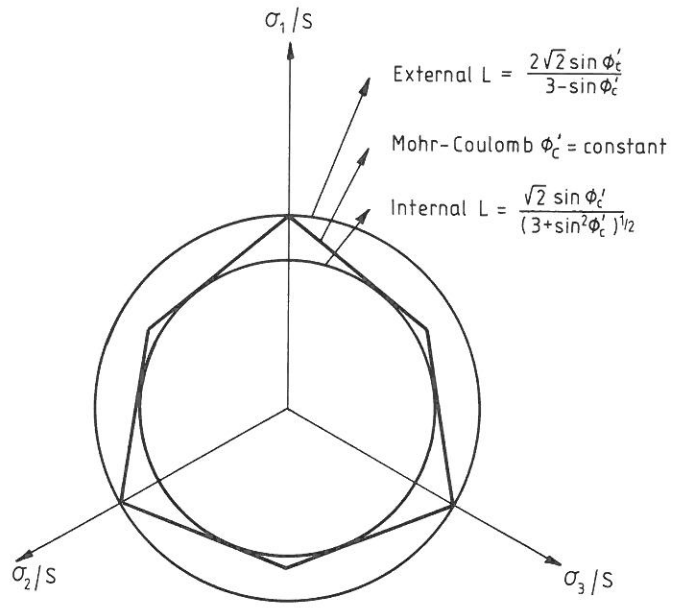

FIG. 2. Mohr-Coulomb with External and Internal Cones

stress path given by $\theta = -23.58°$, falling only slightly to 48.59° in triaxial extension ($\theta = -30°$). The well-known singularity (Bishop 1966) of this surface is also shown in Fig. 3, which occurs when the cone is fitted to a triaxial compression friction angle given by

$$\phi'_c = \arcsin(0.6) = 36.87° \quad \ldots\ldots (16)$$

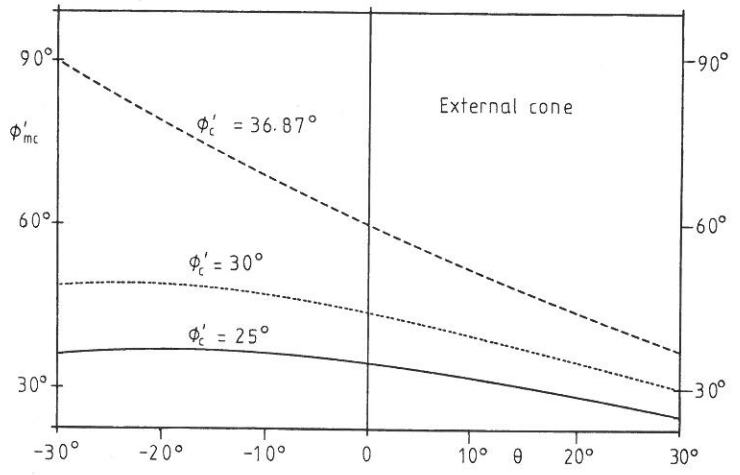

FIG. 3. Equivalent Friction Angle Variation for Three External Cones

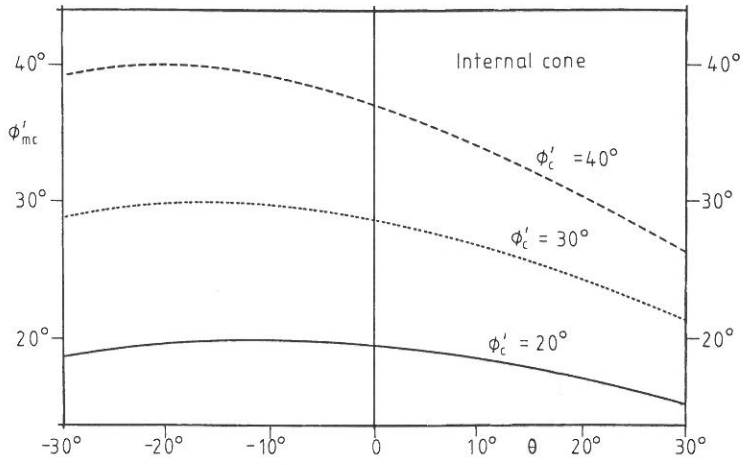

FIG. 4. Equivalent Friction Angle Variation for Three Internal Cones

In this case an infinite shear strength is predicted in triaxial extension as indicated by $\phi'_{mc} = 90°$. The external cone is clearly an unacceptable failure surface for frictional soil.

Internal Cone

Referring to Fig. 2, the internal cone is internally tangent, and hence represents a lower-bound circular fit to the Mohr-Coulomb surface. This surface will clearly predict equivalent friction angles that are less than or equal to the that of the surrounding Mohr-Coulomb surface for all possible stress paths. The radius of the internal cone as viewed in a deviatoric plane is given by

$$L = \frac{\sqrt{2}\sin\phi'_c}{(3 + \sin^2\phi'_c)^{1/2}} \quad \ldots\ldots (17)$$

where ϕ'_c is the friction angle of the surrounding Mohr-Coulomb surface. The point of tangency of the two surfaces is readily shown to occur at the angular location given by (Griffiths 1986)

$$\theta = \arctan\left[\frac{-\sin\phi'_c}{\sqrt{3}}\right] \quad \ldots\ldots (18)$$

Substituting L into Eq. 12 gives the following expression relating the equivalent friction angle ϕ'_{mc} to the angular invariant θ.

$$\phi'_{mc} = \arcsin\left[\frac{\sqrt{3}\sin\phi'_c\cos\theta}{(3 + \sin^2\phi'_c)^{1/2} + \sin\phi'_c\sin\theta}\right] \quad \ldots\ldots (19)$$

Due to the sixfold symmetry in stress space, this relationship is illustrated in Fig. 4 over a 60° sector for three internal cones fitted to $\phi'_c = 20°$, 30°, and 40°. As expected, the maximum value of ϕ'_{mc} occurs at a value of θ given by Eq. 18. Although the internal cone will always give conservative

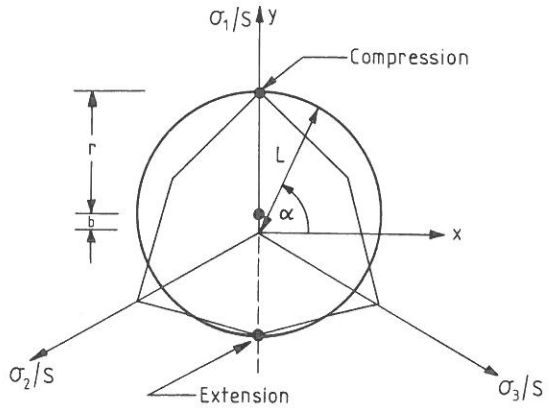

FIG. 5. Anisotropic Cone Fitted to Mohr-Coulomb

estimates of soil strength, certain stress paths produce unacceptably pessimistic predictions. For example, a cone internally tangent to Mohr-Coulomb with $\phi'_c = 40°$ would predict an equivalent friction angle as low as $\phi'_{mc} = 26.39°$ in triaxial compression ($\theta = 30°$).

Anisotropic Cone

An anisotropic cone is shown in Fig. 5 relative to a typical Mohr-Coulomb surface to which it might be fitted. This cone is symmetrical about the σ_1/s axis, hence, due to the twofold symmetry, a 180° sector must be considered. It may also be noted that the use of this surface implies that the principal stresses can be considered as completely independent coordinates, rather than the usual restriction in which

$$|\sigma_1| \geq |\sigma_2| \geq |\sigma_3| \quad \ldots\ldots (20)$$

The cone is fitted to Mohr-Coulomb at the same friction angle ϕ'_c in both extension and compression along the σ_1/s axis, and intersects the hexagon at two other locations on each side of the line of symmetry. The cone will clearly overestimate the Mohr-Coulomb strength for the majority of stress paths, but for some stress paths adjacent to the σ_2/s and σ_3/s axes, the cone will actually underestimate the Mohr-Coulomb strength. As shown in Fig. 5, angular positions in the deviatoric plane are measured using the angle α, which varies in the range $\pm 90°$ and is defined as

$$\alpha = \arctan\frac{y}{x} \quad \ldots\ldots (21)$$

where

$$x = \frac{1}{\sqrt{2}s}(\sigma_2 - \sigma_3) \quad \ldots\ldots (22)$$

and

$$y = \frac{1}{\sqrt{6}s}(2\sigma_1 - \sigma_2 - \sigma_3) \quad \ldots\ldots (23)$$

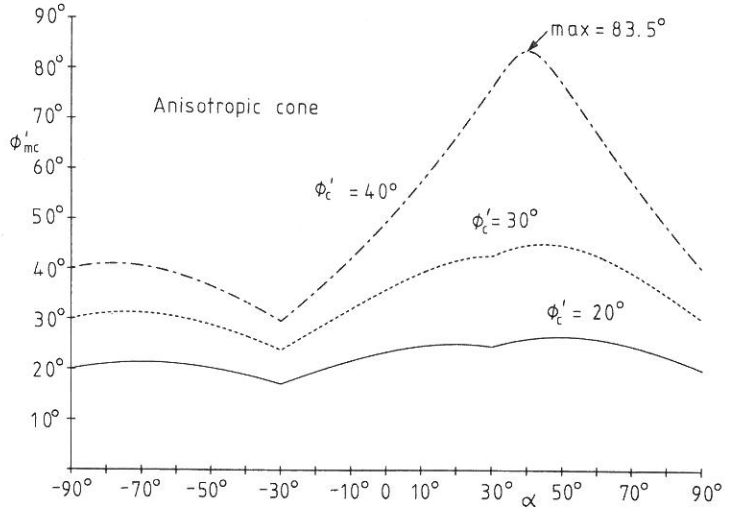

FIG. 6. Equivalent Friction Angle Variation for Three Anisotropic Cones

The radius of the circle is given by

$$r = \frac{6\sqrt{2}\sin\phi'_c}{9 - \sin^2\phi'_c} \quad \ldots\ldots (24)$$

and the distance of its center from the origin by

$$b = \frac{2\sqrt{2}\sin^2\phi'_c}{9 - \sin^2\phi'_c} \quad \ldots\ldots (25)$$

Hence, the distance of the circumference of the circle from the origin can be written as

$$L = b\sin\alpha + [r^2 - b^2\cos^2\alpha]^{1/2} \quad \ldots\ldots (26)$$

Substitution of L into Eq. 12, and noting the substitutions that are necessary between α and θ, gives a function of the form

$$\phi'_{mc} = f(\phi'_c, \alpha) \quad \ldots\ldots (27)$$

This function is plotted in Fig. 6 for three anisotropic cones fitted to $\phi'_c = 20°$, 30°, and 40°. It is clear that serious overestimations of strength are possible. For example, a cone fitted to Mohr-Coulomb at $\phi'_c = 40°$ would predict an equivalent friction angle as high as 83.5° for a stress path given by $\alpha = 39.7°$. As with the external cone, a singularity occurs (Griffiths and Prevost 1988) in the function described by Eq. 27 giving an equivalent friction angle of 90°. This situation arises when

$$\phi'_c = \arcsin(\sqrt{7} - 2) = 40.22° \quad \ldots\ldots (28)$$

and

$$\alpha = \arctan\left[\frac{\sqrt{3}(7\sqrt{7} - 17)}{9(3 - \sqrt{7})}\right] = 39.55° \quad \ldots\ldots (29)$$

Smooth Approximations to Mohr-Coulomb

Although simple geometrically, the circular cones have given very poor representations of soil strength. A more rational approach is to find a failure criterion without corners, based on shear-strength data obtained from a true triaxial device. Two such surfaces are now considered, both of which are supported by experimental evidence produced by their authors.

Lade and Duncan Failure Criterion

This surface, shown in Fig. 7, coincides with Mohr-Coulomb in triaxial compression, but runs outside the hexagon for all other stress paths. The criterion is expressed in invariant form as follows.

$$\frac{I_1^3}{I_3} = K_L \quad \ldots\ldots (30)$$

where

$$K_L = \frac{(3 - \sin\phi'_c)^3}{(1 + \sin\phi'_c)(1 - \sin\phi'_c)^2} \quad \ldots\ldots (31)$$

As before, because of the sixfold symmetry, only a 60° sector needs to be considered. By substituting for I_1 and I_3 from Eq. 11, and replacing σ_2 by the following expression in terms of σ_1, σ_3 and θ

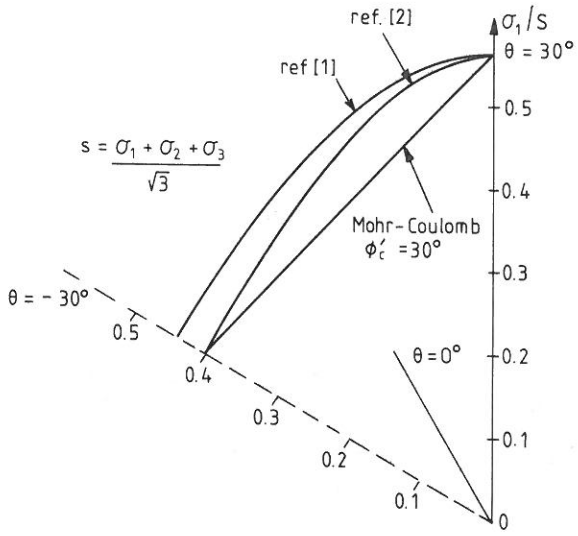

FIG. 7. Lade and Duncan, and Matsuoka and Nakai Surfaces in Relation to Mohr-Coulomb ($\phi'_c = 30°$)

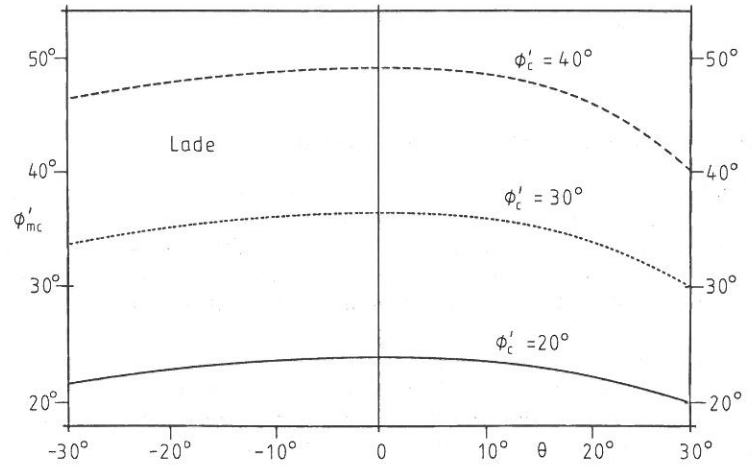

FIG. 8. Equivalent Friction Angle Variation for Three Lade Surfaces

$$\sigma_2 = \frac{\sigma_3}{2}\left[\frac{\sigma_1}{\sigma_3}(1 - \sqrt{3}\tan\theta) + (1 + \sqrt{3}\tan\theta)\right] \quad \ldots\ldots (32)$$

rearrangements lead to a cubic in terms of the Mohr-Coulomb stress ratio at failure R (Eqs. 1–3), thus

$$a_0 + a_1R + a_2R^2 + a_3R^3 = 0 \quad \ldots\ldots (33)$$

where

$$a_0 = 27 + 27\sqrt{3}\tan\theta + 27\tan^2\theta + 3\sqrt{3}\tan^3\theta \quad \ldots\ldots (34a)$$

$$a_1 = (81 - 4K_L) - \sqrt{3}(4K_L - 27)\tan\theta - 27\tan^2\theta - 9\sqrt{3}\tan^3\theta \quad \ldots\ldots (34b)$$

$$a_2 = (81 - 4K_L) + \sqrt{3}(4K_L - 27)\tan\theta - 27\tan^2\theta + 9\sqrt{3}\tan^3\theta \quad \ldots\ldots (34c)$$

$$a_3 = 27 - 27\sqrt{3}\tan\theta + 27\tan^2\theta - 3\sqrt{3}\tan^3\theta \quad \ldots\ldots (34d)$$

By choosing a value of ϕ'_c which fixes K_L, the cubic can be solved for R over the range $-30° \le \theta \le 30°$. It may be noted that every time the cubic is solved, only one of the three roots is relevant. When this root is found, the equivalent friction angle ϕ'_{mc} is easily back-figured from Eq. 35, thus

$$\phi'_{mc} = 2\arctan\sqrt{R} - 90° \quad \ldots\ldots (35)$$

The variation of ϕ'_{mc} with θ is shown in Fig. 8 for three Lade surfaces corresponding to $\phi'_c = 20°$, 30°, and 40°. As expected, the surfaces coincide with Mohr-Coulomb when $\theta = 30°$, but run outside it for all other stress paths. For example, when the Lade surface is fitted to Mohr-Coulomb at $\phi'_c = 40°$, a maximum equivalent friction angle of 48.9° is reached at $\theta = 0°$, falling to 46.2° in triaxial extension ($\theta = -30°$).

Matsuoka and Nakai (1974) Failure Criterion

This surface, also shown in Fig. 7, coincides with Mohr-Coulomb at all apexes corresponding to triaxial extension and compression. The relationship

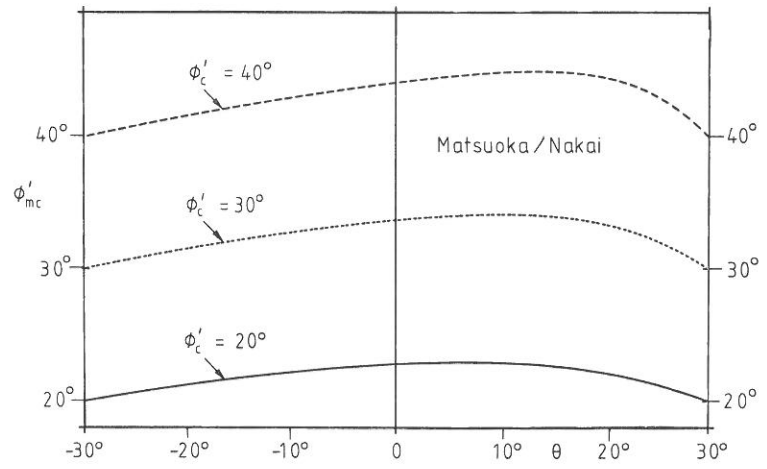

FIG. 9. Equivalent Friction Angle Variation for Three Matsuoka and Nakai Surfaces

between this surface and Mohr-Coulomb is analogous to that between von-Mises and Tresca. The criterion is expressed in invariant form as follows.

$$\frac{I_1I_2}{I_3} = K_{MN} \quad \ldots\ldots (36)$$

where

$$K_{MN} = \frac{9 - \sin^2\phi'_c}{1 - \sin^2\phi'_c} \quad \ldots\ldots (37)$$

By substitution of I_1, I_2, I_3, and σ_2 from Eqs. 11 and 32, a cubic of the type given in Eq. 33 is obtained, but with the rather simpler coefficients given by

$$a_0 = 3 + 4\sqrt{3}\tan\theta + 3\tan^2\theta \quad \ldots\ldots (38a)$$

$$a_1 = (15 - 2K_{MN}) - 2\sqrt{3}(K_{MN} - 3)\tan\theta - 3\tan^2\theta \quad \ldots\ldots (38b)$$

$$a_2 = (15 - 2K_{MN}) + 2\sqrt{3}(K_{MN} - 3)\tan\theta - 3\tan^2\theta \quad \ldots\ldots (38c)$$

$$a_3 = 3 - 4\sqrt{3}\tan\theta + 3\tan^2\theta \quad \ldots\ldots (38d)$$

By choosing a value of ϕ'_c that fixes K_{MN}, the cubic can be solved for R in the range $-30° \le \theta \le 30°$ and the equivalent friction angle back-figured from Eq. 35. Typical values are shown in Fig. 9 for three Matsuoka Nakai surfaces corresponding to $\phi'_c = 20°$, 30°, and 40°. As expected, the surfaces coincide with Mohr-Coulomb in both triaxial positions ($\theta = \pm 30°$) and reach a maximum at an intermediate location. For example, if the Matsuoka Nakai surface is fitted to Mohr-Coulomb at $\phi'_c = 40°$, a maximum equivalent friction angle of 44.93° is reached at $\theta = 13°$.

Not only is this surface more conservative than Lade's for all stress paths, but the maximum value of ϕ'_{mc} occurs at a different location. In the Lade

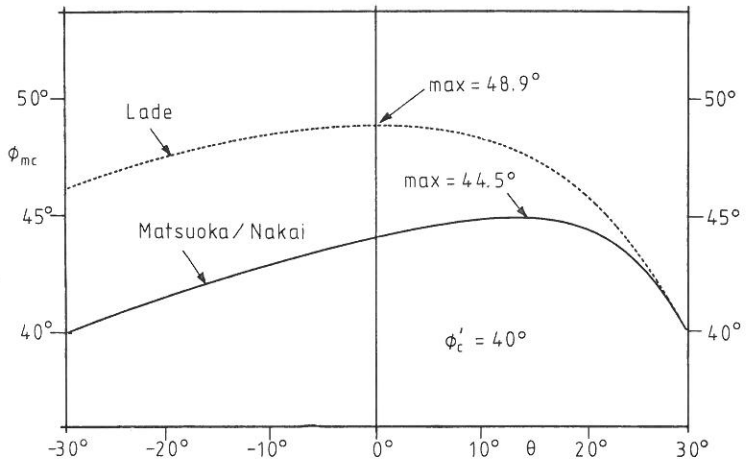

FIG. 10. Lade and Duncan, and Matsuoka and Nakai Surfaces Fitted at ($\phi_c' = 40°$)

surface, the maximum always occurs at $\theta = 0°$, whereas in the Matsuoka Nakai surface, the maximum depends on ϕ_c'. For comparison, both surfaces corresponding to $\phi_c' = 40°$ are shown together in Fig. 10. It can be noted from this figure that even these sophisticated surfaces predict equivalent Mohr-Coulomb friction angles that differ by as much as 6° in triaxial extension. To put this in perspective, under plane strain conditions a change in the friction angle of 4° from 44° to 48° causes the predicted bearing capacity of a strip footing to increase by a factor of three (Lambe and Whitman 1969)!

Conclusions

A unified approach to the portrayal of failure criteria for cohesionless soils has been presented. The method has enabled various failure criteria to be expressed in terms of an equivalent Mohr-Coulomb friction angle varying as a function of the angular invariant. This approach has been used so that some of the failure criteria currently being used in finite element analyses of boundary value problems can be interpreted in terms of the familiar Mohr-Coulomb friction angle. A convenient form of dimensionless principal stress space has been used to illustrate the differences between the criteria.

Circular conical surfaces, although convenient geometrically, were shown to contain singularities and lead to considerable variations in predicted soil strength, depending on the stress path followed.

Noncircular conical approximations to Mohr-Coulomb were also considered. These surfaces are preferred, as they are based on actual soil data. However, their interpretation in terms of a friction angle requires the solution of cubic equations. It was noted that even the sophisticated surfaces based on carefully conducted triaxial tests could differ by several degrees when so interpreted. Such differences in the case of a bearing-capacity problem could lead to predictions differing by up to a factor of three for surfaces fitted to Mohr-Coulomb at 40°.

For analyses involving materials whose friction angles lie in this range,

the Mohr-Coulomb criterion remains attractive on the grounds of its simplicity and conservatism.

Appendix I. References

Bishop, A. W. (1966). "The strength of soils as engineering materials: 6th Rankine lecture." *Géotechnique,* 16(2), 91–130.

Drucker, D. C., Gibson, R. E., and Henkel, D. J. (1957). "Soil mechanics and work-hardening theories of plasticity." *Trans. of the American Society of Civil Engineers,* 122, 338–346.

Drucker, D. C., and Prager, W. (1952). "Soil mechanics and plastic analysis in limit design." *Quart. Appl. Mech.,* 10, 157–165.

Griffiths, D. V. (1986). "Some theoretical observations on conical failure criteria in principal stress space." *Int. J. Solids Struct.,* 22(5), 553–565.

Griffiths, D. V., and Prevost, J. H. (1988). "The properties of anisotropic conical failure surfaces in relation to the Mohr-Coulomb criterion." *Int. J. Numer. Anal. Methods Geomech.,* 12(5), 497–504.

Humpheson, C. (1976). "Finite element analysis of elasto/viscoplastic soils," thesis presented to the University of Wales, at Swansea, Wales, in partial fulfillment of the requirements for the degree of Doctor of Philosophy.

Lade, P. V., and Duncan, J. M. (1975). "Elasto-plastic stress-strain theory for cohesionless soils." *Proc.* American Society of Civil Engineers, 101(10), 1037–1053.

Lambe, T. W., and Whitman, R. V. (1969). "Soil Mechanics, John Wiley and Sons, New York, N.Y., 206.

Matsuoka, H., and Nakai, T. (1974). "Stress-deformation and strength characteristics of soil under three different principal stresses." *Proc.* Japanese Society of Civil Engineers, 232, 59–70.

Mroz, A. (1967). "On the description of anisotropic work hardening." *J. Mech. Phys. Sci.,* 15, 163–175.

Prevost, J. H. "A simple plasticity theory for frictional cohesionless soils." Soil Dyn. Earthquake Engrg., 4(1), 9–17.

Smith, I. M. (1988). "Two 'class A' predictions of offshore foundation performance," G. Swoboda, ed., *Proc. 6th Int. Conf. on Numerical Methods in Geomechanics,* A. A. Balkema, Rotterdam, The Netherlands, 137–144.

Smith, I. M., and Griffiths, D. V. (1988). *Programming the Finite Element Method.* 2nd Ed., John Wiley and Sons, New York, N.Y.

Vermeer, P. A. (1978). "A double hardening model for sand." *Géotechnique,* 28(4), 413–433.

Zienkiewicz, O. C., et al. (1978). "A unified approach to the soil mechanics of offshore foundations," *Numerical methods in offshore engineering,* John Wiley and Sons, New York, N.Y., 361–412.

Appendix II. Notation

The following symbols are used in this paper:

$a_0, \ldots a_3$ = coefficients in cubic expressions;
b = distance of circle center from origin;
$I_1, \ldots I_3$ = stress invariants;
K_L = constant associated with Lade and Duncan criterion;
K_{MN} = constant associated with Matsuoka and Nakai criterion;
K_p = passive earth pressure coefficient;
L = dimensionless shear stress level (t/s);
R = principal stress ratio at failure (σ_1/σ_3);
r = radius of circle;
s = mean stress invariant;

t = shear-stress invariant;
x, y = Cartesian coordinates;
α = angular measure in stress space;
θ = lode angle;
$\sigma_1, \ldots \sigma_3$ = principal stresses;
ϕ'_c = friction angle in triaxial compression; and
ϕ'_{mc} = equivalent Mohr-Coulomb friction angle.